GEOLOGIC MAP OF THE CENTRAL FAR SIDE OF THE MOON

By
Desiree E. Stuart-Alexander

1978

Prepared for the
National Aeronautics and Space Administration
by
U.S. Department of the Interior, U.S. Geological Survey

(Published in hardcopy as USGS Miscellaneous Investigations Series Map I–1047, as part of the Geologic Atlas of the Moon, 1:5,000,000 Series. Hardcopy is available for sale from U.S. Geological Survey, Information Services, Box 25286, Federal Center, Denver, CO 80225)

Please direct questions or comments about the digital version to:
Richard Kozak
U.S. Geological Survey
2255 N. Gemini Drive
Flagstaff, AZ 86001
e-mail: rkozak@flagmail.wr.usgs.gov

DESCRIPTION OF MAP UNITS

CRATER MATERIALS

(Only craters 20 km or more in diameter are mapped)

Cc MATERIAL OF VERY SHARP-RIMMED RAYED CRATERS

Ec MATERIAL OF SHARP-RIMMED CRATERS

Ic_2 MATERIAL OF SINGLE CRATERS—Orientale basin age or younger

Ic_1 MATERIAL OF SINGLE CRATERS—Older than Orientale basin and younger than Imbrium basin

Ic MATERIAL OF IMBRIAN CRATERS, UNDIVIDED

Ico MATERIAL OF ELONGATE CLUSTERS OF CRATERS APPROXIMATELY RADIAL TO ORIENTALE BASIN—*Interpretation:* secondary craters of the Orientale basin

Icc MATERIAL OF ELONGATE AND IRREGULAR CLUSTERS OF CRATERS—Some not obviously related to any particular Imbrian basin or crater, others secondary craters of adjacent Imbrian crater to which they are approximately radial

Ifc FURROWED, RAISED CRATER FLOOR OR FILL MATERIAL—Most are convex upward. Texture equally sharp in Nectarian and Imbrian craters. *Interpretation:* postimpact filling, probably lava

Nc MATERIAL OF SUBDUED CRATERS—Older than Imbrium basin and younger than Nectaris basin

Ncc MATERIAL OF ELONGATE CLUSTERS OF SUBDUED CRATERS—Craters approximately the same size. *Interpretation:* secondary craters of the Nectarian basin to which they are adjacent and (or) approximately radial

pNc MATERIAL OF SUBDUED TO VERY SUBDUED CRATERS—Older than Nectaris basin

BASIN MATERIALS

(Multiringed circular structures 300 km or more in diameter as measured across most prominent ring)

Nb MATERIAL OF RAISED RIMS AND SLUMPED WALLS OF BASINS—Primarily the outermost ring. *Interpretation:* disrupted bedrock largely covered by ejecta

Nbl LINEATED MATERIAL SURROUNDING BASINS—Linear elements approximately radial to basin; locally only weakly developed. *Interpretation:* basin ejecta deposited ballistically and as massive flows

NpNbm MATERIAL OF NECTARIAN BASIN MASSIFS—Massive mountain blocks, mainly form part of outermost basin rings; inner ring in Korolev. *Interpretation:* uplifted and structurally complex blocks of prebasin bedrock; may be covered by basin ejecta

NpNbr MATERIAL OF RUGGED MOUNTAINS AND MOUNTAIN SEGMENTS OF NECTARIAN BASINS—Smaller than massifs (unit NpNbm); mainly form

inner rings. *Interpretation:* uplifted and complexly faulted prebasin bedrock; may be covered by basin ejecta

pNb PRE-NECTARIAN BASIN MATERIAL, UNDIVIDED—Subdued, eroded mountain rings and arcuate segments of rings

pNbm MATERIAL OF PRE-NECTARIAN BASIN MASSIFS—Relatively massive single mountain blocks or part of continuous ring. *Interpretation:* same as unit NpNbm

pNbr RUGGED MATERIALS OF PRE-NECTARIAN BASINS—Discontinuous blocky mountains forming arcuate ring segments; smaller than massifs (unit pNbm). *Interpretation:* same as unit NpNbr

OTHER MATERIALS

Ip MARE MATERIALS OF DARK PLAINS—*Interpretation:* basaltic lavas, by analogy with returned Apollo samples. STIPPLED PATTERN: light streaks and swirls in Mare Ingenii. *Interpretation:* Surficial markings of uncertain origin, probably not related to underlying mare rocks

INp MATERIAL OF GROOVES AND MOUNDS—Covers craters and other terrae of pre-Nectarian through Imbrian age. Craters have mainly radial grooves on rim and walls; some mounds Level terra has mounds and grooves. Particularly well developed around Mare Ingenii and crater Van de Graaff. *Interpretation:* origin uncertain; general area antipodal to Imbrium basin; therefore could be depositional site of Imbrium ejecta that traveled around the Moon, or mass-wasting caused by Imbrium seismic shaking; alternatively, may be some unidentified local phenomenon unique to this area

Np SMOOTH LIGHT PLAINS—Generally higher density of craters than on maria. *Interpretation:* may be related to formation of an Imbrian basin

INp LIGHT PLAINS—Higher density of craters than unit Ip. *Interpretation:* may be related to various Imbrian and/or Nectarian basins

Np HIGHLY CRATERED LIGHT PLAINS—*Interpretation:* may be related to Nectarian basins

It RELATIVELY FRESH-APPEARING, IRREGULAR TERRA—Low relief; low density of superposed craters. *Interpretation:* probably a complex mixture of local erosional debris and crater and basin ejecta

Nt ROLLING TERRA—Moderately high density of craters, particularly craters of diameter less than 20 km. *Interpretation:* same as unit It

NpNt IRREGULAR TERRA—Covers large areas and has high density of craters larger than 20 km wide. *Interpretation:* same as unit It

pNt CRATERED TERRA—High density of arcuate low hills or crater segments, and pre-Nectarian craters. *Interpretation:* same as unit It except contains erosional remnants of pre-Nectarian craters

CORRELATION OF MAP UNITS

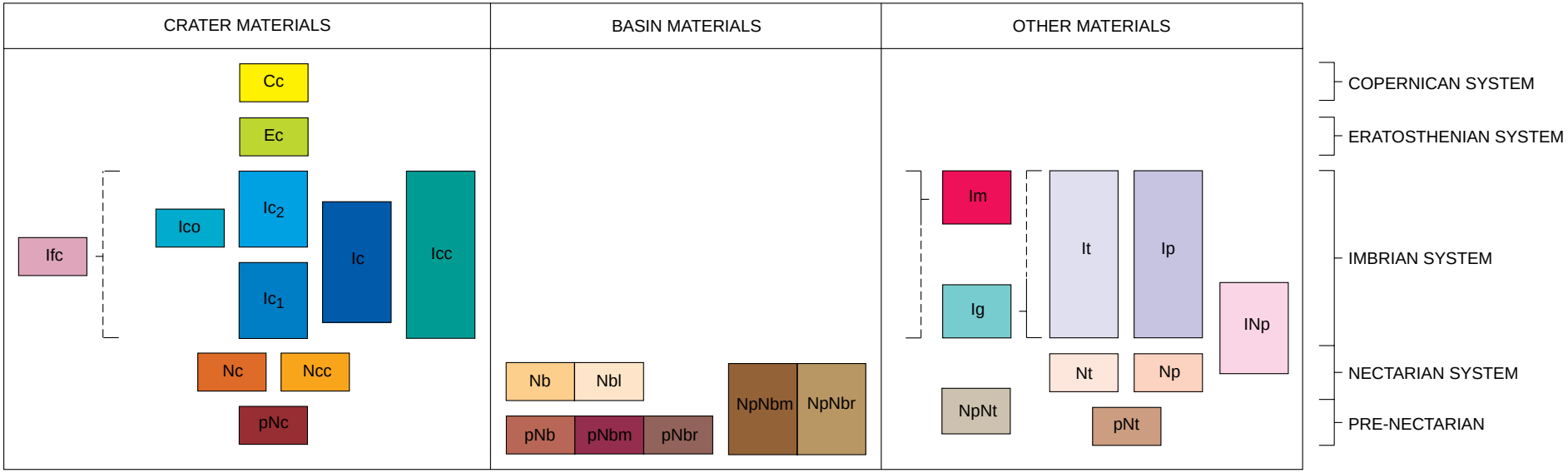

Contact

Generalized crest of basin ring structure

Slope—Drawn at base of steep slope; barb points down slope


Covered crater rim crest

INTRODUCTION

This map is one of a series of geologic maps that will cover the entire Moon at a scale of 1:5,000,000[1] The geology of the central far side is compiled largely from NASA Lunar Orbiter and Apollo photographs and Soviet Zond photographs; the discussion and interpretation of geologic units incorporate the geochemical and geophysical data obtained from orbiting spacecraft. Geologic units are based on the stratigraphic framework established by Shoemaker and Hackman (1962) as subsequently revised (summarized by McCauley, 1967; Wilhelms, 1970; Mutch, 1972; Stuart-Alexander and Wilhelms, 1975). Description of map units is brief because they largely follow units described on the nearside 1:5,000,000 map of Wilhelms and McCauley (1971). The reader unfamiliar with lunar maps, mapping principles, and terminology is referred to that map. Only new units and features or units whose origins are still much in doubt are discussed here.

GEOLOGIC SUMMARY

GENERAL FEATURES

Broad geologic patterns, formed primarily by the arrangement and relative abundance of units common to all provinces, divide the central lunar far side into four general provinces. The most diversified province fills the southern third of the mapped area and is coincident with a nearly obliterated pre-Nectarian basin, here named the South Pole–Aitken basin for two landmarks along its rim. Within this basin is the largest far-side concentration of maria and light plains and also the unique occurrence of a strangely grooved material (unit Ig). Ringing the basin and locally covering it is a province consisting of a wide band of pre-Nectarian cratered terra (unit pNt). Two provinces constitute the northern half of the map area: a zone of nondescript irregular terra (unit NpNt) occupies most of it, and a smaller, irregular patch of pre-Nectarian cratered terra (unit pNt) occurs along the north-east to north-central border of the area. Key features within all provinces are the multiringed circular basins and some areally restricted terra and plains units. An unrelenting rain of bolides produced the shotgun pattern of craters randomly superposed over the entire map area.

PRE-NECTARIAN MATERIALS

The oldest discernible structures are subdued mountain remnants of the South Pole–Aitken basin. The northernmost chain of mountains (lat 16° S., long 160–170° W.) was first recognized on Apollo 8 photographs but was not thought to be associated with any basin (Wilhelms and others, 1969). Extensive detailed mapping now shows that this chain is the largest of several linear mountains scattered around the periphery of a giant depression. A line drawn through these mountains describes a crude circle centered at about lat 50° S., long 180° W. near the crater Von Kármán. K. A. Howard and H. G Wilshire (written commun., 1976) have identified several isolated mountains that continue the skeletal outlines of this great basin, including mountains at lats 80° S. and 85° S. that locate a possible southern boundary. Also, Wilhelms and El-Baz (1977) have mapped some isolated mountains at lat 38° S. long 130° E. that probably mark the western limits of the basin. In order to include these mountains in the circumference of the basin, I have drawn on this map a generalized basin ring north of the western mountain segments near the crater O'Day. Projecting the ring in a circle southward would include the mountains near the South Pole and give the basin a diameter of about 2,000 km, making it about 700 km larger than the Imbrium basin (Markov, 1962; Hartmann and Kuiper, 1962; Stuart-Alexander and Howard, 1970; Hartmann and Wood, 1971).

---

[1] The series is an outgrowth of the original 1:1,000,000 quadrangle maps constructed for the nearside in support of the unmanned and Apollo spaceflight programs (Wilhelms, 1970).

A topographic low in the area of the South Pole–Aitken basin was first identified from Zond photographic altimetry (Rodionov and others, 1971) and confirmed by Apollo laser altimetry. The photographic measurements were made about 10° east of the center of the basin as mapped here and intersected a segment of about 60° of longitude (1,800 km). Apollos 15 and 17 crossed the northern segment of the basin and furnished detailed topographic profiles along a narrow strip (Wollenhaupt and Sjogren, 1972a; Wollenhaupt and others, 1973). The terrain within the northern segment is highly irregular (fig. 1), both because of the high density of superposed craters and because of the uneven mountain segments that form the residual rings of this large basin. The photographic data are more generalized than the laser data and show the average basin depth to be 5 to 6 km below the central far-side terra and more than 7 km below the southern near-side terra along long 10°E. The most recent compilations of laser altimetry also show that the lowest areas within the basin are as deep as any on the near side of the Moon and more than 6 km below the adjacent highlands (Kinsler and others, 1975; Bills and Ferrari, 1975).

The second oldest feature mapped is a smaller basin in the northern irregular terra province. The basin is centered at lat 19° N., long 175 E., near the crater Buys-Ballot and small patches of maria. It is here named the Freundlich-Sharonov basin for two conspicuous superposed craters. The western mountains of this basin were first reported by Campbell, O'Leary, and Sagan (1969) and Baldwin (1969). The eastern perimeter is identified by well-developed, arcuate scarps that face basinward. As mapped here, the basin is 600 km in diameter, although Baldwin (1969) considered these outermost mountains to be inner rings. His postulated outer two rings at 1,000 km and 1,600 km are not confirmed; in fact, the laser altimetry from Apollo 16 (Wollenhaupt and Sjogren, 1972b) shows topographic highs in areas that should be intermountain lows if any outer rings had existed.

The remaining pre-Nectarian materials comprise two additional basins, many craters, and heavily cratered terra. One basin, Apollo, lies entirely within the South Pole–Aitken basin. The other, here named the Keeler–Heaviside basin for the two craters that almost fill it, lies immediately north of the South Pole–Aitken basin and within the southern province of old terra (unit pNt). This province surrounds and locally penetrates the South Pole–Aitken basin, supporting the great antiquity of that basin. The northern province of old terra (unit pNt) is much more irregular and does not seem to be related to any structure. The terra consists of rolling, rough terrain because much of it is arcuate hillocks that are probably remnants of old battered craters.

The irregular terra (unit NpNt) is considered to contain both pre-Nectarian and Nectarian materials. Fewer pre-Nectarian features lie within its limits than within the older terra, the unit is probably a mixture of ejecta from Nectarian and pre-Nectarian basins and craters. It undoubtedly contains admixtures of even younger ejecta, but these do not show. The unit forms monotonous, uneven, rolling ground. The physical nondistinctiveness of this terra is paralleled by the geochemical monotony of the terrain as discussed below.

NECTARIAN SYSTEM

In general, Nectarian units correspond in kind to those of the pre-Nectarian and therefore are interpreted as products of similar processes. The main differences occur in the random distribution of a major Nectarian units and in the smaller average size of Nectarian basins relative to pre-Nectarian ones. Also, certain physical differences are apparent because of the comparative youthfulness of Nectarian features. Not only are details such as crater rim-crests a little sharper, but the texture of parts of ejecta blankets around Nectarian basins is sufficiently distinct to permit mapping them as a lineated unit (Nbl), separate from the basin rims (units Nb and NpNbr).

Within the Nectarian System are the oldest discernible units among the light plains materials that cover approximately 5 percent of the lunar surface. Nectarian highly cratered light plains (unit Np) are scattered across the map area as fillers in a few basins and large craters. More abundant are the light plains mapped here as consisting of both Imbrian and

Nectarian materials (unit INp), but most abundant are the Imbrian plains which form 4 percent of the lunar surface (Howard and others, 1974, p. 319). Eratosthenian and Copernican plains exist, but none are identified at the scale of this map. The comparative scarcity of Nectarian plains may not be due to lack of original plains materials but rather to their destruction by impact and perhaps other processes that tend to roughen smooth surfaces.

Leading contending theories of the origin of light plains seem to be those that relate the plains to basin formation. By one theory they form from the lateral transport of fluidized ejecta (Eggleton and Schaber, 1972); by another they form from ballistic transport of ejecta (for example, Moore and others, 1974; Chao, 1974); and by another they are primarily erosional in origin, consisting of mass wasted material and of local material that has been reworked and redeposited by secondary craters of distant craters or basins (Oberbeck and others, 1974, 1975). An earlier concept was that the light, smooth plains were predominantly very fluid lavas or pyroclastic rocks (for example, Milton and Hodges, 1972; Trask and McCauley, 1972), but rocks from the plains sampled by the Apollo astronauts were predominantly impact-brecciated plagioclase-rich rocks (Apollo 16 Preliminary Examination Team, 1973).

IMBRIAN SYSTEM

Contrasts between Imbrian and older features indicate that the Imbrian Period was a time of transition in the history of the Moon. One of the changes occurred in the influx of large bolides, which is reflected in the relative numbers of large craters in each lunar system. There are only three Imbrian basins on the entire Moon, none of which is in this map area where the largest Imbrian crater is only about 145 km in diameter. Here there are 14 Imbrian craters 100 km or more across, 38 Nectarian craters, and 47 pre-Nectarian. Whether or not impacts of this size reached a steady state (Baldwin, 1969; Howard and others, 1974), younger craters and basins have obliterated older ones, so that 47 is a minimum count for the pre-Nectarian.

Despite the discrepancy in numbers of large impact features, the maximum time available for the pre-Nectarian and Nectarian combined (Tera and others, 1974; Stuart-Alexander and Wilhelms, 1975) about equal to the minimum length of the Imbrian Period, that is, roughly 600 m.y., assuming that the top of the Imbrian lies within the timespan of the deposition of the Apollo 15 mare basalts (Carr and El-Baz, 1971). The absolute age for those basalts is 3.3 ± 0.1 g.y (Papanastassiou and Wasserburg, 1973), leaving three-quarter of all lunar history with no basins.

Another change within the Imbrian Period is a reduction in the flux rate for smaller craters. This change is less dramatic than differences in numbers of basins but is important and has been well documented (for example, Soderblom and Lebofsky, 1972; Boyce and others, 1974).

Another transition in lunar evolution is recorded by the plains units, which form an important part of the Imbrian record. The oldest mare basalts (dark plains, unit Im) that have been recognized belong to the Imbrian System (Stuart-Alexander and Howard, 1970); they may be younger than the Orientale basin (Wilhelms, 1970; Wilhelms and McCauley, 1971). Maria on the central far side are harder to date stratigraphically than those on the near side because they form in isolated patches that are not in contact with easily distinguishable Orientale or Imbrium basin materials. The far-side mare appear to be lighter (higher albedo) than most near-side maria, possibly the result of lightening with age (Stuart-Alexander and Howard, 1970) or alternatively perhaps slight differences in chemical composition.

Imbrian smooth light plains (unit Ip) are scattered across the area but appear to be somewhat more abundant in the east half to two-thirds. As this is the region closest to Orientale, a control by that basin is possible, as noted by Howard, Wilhelms, and Scott (1974) and Scott and others (1977). The Concentration here is greatest in and around the basins Korolev and Apollo, which, while closest to Orientale, are not directly in line with

the major extent of the Orientale ejecta blanket as mapped by Scott and others (1977). There is a slight concentration of light plains in the northeast, where most of the identified Orientale secondaries (unit Ico) occur, but there is no preferred juxtaposition or other apparent relation between the secondaries and the light plains. Therefore, this mapping does not resolve the origin of light plains.

Origin of the unit of grooves and mounds (Ig) is uncertain. No other lunar terrain is exactly like it. Its features are sharper than those of "hilly and pitted terrain" (Wilhelms and McCauley, 1971; Wilhelms and El-Baz, 1977) and its positive elements less regular than those of "hilly and furrowed terrain" (Wilhelms and McCauley, 1971). It is more strongly and sharply developed on crater rims and walls than are the other two units. Distribution of the grooves and mounds is limited to an area within the South Pole–Aitken basin from lat 20° S. to 47° S., long 147° E. to 178° W. The largest exposure of the unit covers about 23,000 km^2. The juxtaposition of all exposures suggests a common origin but not necessarily one related to the huge containing basin.

Three proposed explanations for the origin of the grooves and mounds are extrusive volcanism, impact of ejecta from the Imbrium basin, and mass-wasting caused by a shock wave from the Imbrium basin impact. Before Apollo 16 landed at Descartes, some sort of highland volcanism seemed a reasonable explanation for units such as the hilly and furrowed material on the Moon's near side, but only impact-brecciated plutonic rocks were collected there, not volcanic rocks. This does not categorically exclude a volcanic interpretation for terra materials, but it does make them less probable for terrain of similar morphology.

Both hypotheses that stress a relation of the grooved unit to the Imbrium basin do so because of the unit's antipodal position to Imbrium. Similar associations occur elsewhere: an area of furrowed and pitted terrain near Mare Marginis is antipodal to the Orientale basin (Moore and others, 1974; Wilhelms and El-Baz, 1977), and an area of hilly and pitted terrain of Mercury is antipodal to the Caloris basin (Murray and others, 1974, p. 176). Schultz and Gault (1975) have proposed that these features may have formed by extensive mass-wasting caused by seismic waves associated with the impact that produced the basin. P waves and surface waves would eventually converge at the antipodal point, the P waves before arrival of ejecta and the surface waves simultaneously with the ejecta. Reflected tensile waves would converge beneath the antipodal points, adding to disruption of the surface. Moore, Hodges, and Scott (1974, p. 91), however, ascribe the terrain features primarily to convergence of ejecta at the antipodal point. The strongest evidence supporting an impact-related hypothesis comes from the apparent contemporaneity of all parts of the unit; the grooves and mounds seem to be of comparable freshness everywhere yet are superimposed on craters that range in age from pre-Nectarian to uppermost Nectarian (perhaps to lower-most Imbrian).

The physical appearance of the unit suggests that ejecta deposition dominated and that seismic shaking played a subsidiary role. Mounds and grooves out on the level terra are not related to slopes in arrangement or shape as would be expected if they formed by mass wasting. Additionally, in some places material seems to have piled up on top of crater rim crests and some grooves are normal to crater rim crests, suggesting ejecta deposition. However, the down-slope movement of abundant material inside crater walls could have been produced by shaking from ejecta impacting the surface or from seismic waves.

ERATOSTHENIAN AND COPERNICAN SYSTEMS

In the map area, the Eratosthenian and Copernican Systems are only represented by craters 75 km wide or smaller; no other materials were identified. Craters of both systems are randomly distributed. Eratosthenian craters are more abundant than Copernican, corroborating the decline in flux rate proposed by Soderblom and Lebofsky (1972).

GEOCHEMISTRY AND GEOPHYSICS

Significant data have been collected from orbit by Apollos 15, 16, and 17, Zond 6, and lunar Orbiter 5. Results most relevant to the central far side were obtained from laser altimetry, photogrammetric whole-disk altitude measurements, gamma-ray spectroscopy, subsatellite magnetometry, and gravity calculations based on spacecraft perturbations. X-ray fluorescence coverage of the central far side was insufficient for analysis because the data are limited to narrow bands in the westernmost 12° of longitude. Results of other experiments expected to produce useful data should be released in the near future. These include data from infrared thermal emissions, alpha-particle spectrometry, and radar sounding.

ALTIMETRY

Altitude measurements computed by various methods have been compiled by Bills and Ferrari (1975) into a generalized topographic map for a wide belt around the Moon encompassing lat 45° N. to 45° S. Detailed topographic profiles in an east-west direction were provided by the reduction of laser altimetry data recorded by Apollos 15, 16, and 17 (Wollenhaupt and Sjogren, 1972a and b; Wollenhaupt and others, 1973), and in a polar cross section from the photogrammetric altimetry of Zond 6 (Rodionov and others, 1971). Kinsler, Merrill, and Srnka (1975) have prepared a map at a resolution of 1 km of the orbital tracks along which laser altimetry was collected by Apollos 15. 16, and 17.

Comparison of results from the different methods of altimetry are in reasonable agreement once the photogrammetric data have been converted from a geometrically spherical Moon to a Moon spherical about the center of mass. As discussed earlier, both the laser altimeter and photogrammetric limb measurements confirm a major deep depression in the southern hemisphere of the far side (the South Pole–Aitken basin, fig. 1) and show that this depression is as deep as any basin on the near side. Additionally, the laser altimeter indicates that there is a major topographic high north of the basin and east of long 180°. Along the Apollo 16 ground track (fig. 2), the high extends from about 180° to 135° W.; along the Apollo 15 (fig. 1) and 17 ground tracks (Kinsler and others, 1975) it extends from about 155° W. to 125° W. These data suggest that there may be a broad arch, trending northwestward, that averages more than 3 km above a spherical Moon. Unfortunately the photogrammetric data are so poor or nonexistent in a 25° strip (Rodionov and others, 1971) that includes the Apollo 16 ground track that neither the topographic high nor the continuation or termination of the light terrain northward can be confirmed. From the photogrammetric data alone, however, it seems that the terrain north of about lat 25° N. does not rise significantly above the spherical Moon radius (Rodionov and others, 1971). It is significant that the southern near-side highlands, and area not sampled by the Apollo laser altimeter, do appear as a major topographic high in the photogrammetric data .

If the photogrammetric data are correct, as they seem to be, then there are no significant differences in altitudes between the near and far sides, only between basins and nonbasin terra. Altitude differences of 7 km or more exist between the basin deeps and adjacent terra masses. Major near-side and far-side basins seem to be equally deep, and major terra masses rise equally far above the mean radius of the Moon on both hemispheres. This equality suggests that the crust on the southern near-side highlands is as thick as that postulated for the far side by Kaula, Schubert, Lingenfelter, Sjogren, and Wollenhaupt (1973).

GAMMA-RAY SPECTROMETRY

A plot of total lunar radioactivity measured by orbiting gamma-ray spectrometers is included here for the central far side (fig. 3). Selected areas of the whole plot, which covers about 20 percent of the lunar surface (Metzger and others, 1973a, b), have been used to calibrate the orbital values with those at some of the landing sites by Trombka, Arnold, Reedy, and Peterson (1973). They found that the orbital values tend to be higher than the

ground-based measurements but that the trends are in good agreement. The orbital data are averaged over 2° squares, 60 km on a side, and generally show that maria are more radioactive than terrae. Data reduction is still being refined, but it is apparent that there are variations within the terrae, within one mare, and from one mare to another; the western maria on the near side are the most radioactive. Radioactivity on the central far side seems low (fig. 3), except for an anomaly that extends from long 160° E. to 166° W. and includes the Van de Graaff region.

The source of the anomaly is not apparent. It might be caused by the four patches of maria that are spread out under the ground track, but these make up less than 20 percent of the area. Most of the maria lie south of the ground track and should not strongly affect the data. Alternatively, the radioactivity may be related to the grooved terrain (unit Ig), although this terrain does not appear to extend under the easternmost 10° of the anomaly. If this unit were formed by ejecta from the Imbrium basin, it might correlate with the high radioactive values measured on the surface at the Apollo 14 site (Eldridge and others, 1972) and recorded in that general area from orbit by Apollo 16. The terra rocks there have been mapped as Imbrium basin ejecta (Eggleton, 1964, 1965; Wilhelms and McCauley, 1971).

Further analysis of the gamma-ray data has resulted in preliminary values for concentrations of iron, magnesium, and titanium as well as separate values for potassium and thorium plus uranium, rather than total radioactivity. These concentrations have been published (Metzger and others, 1974) using generally fairly large resolution cells (fig. 4) for the preliminary analysis. The main far-side highland areas—B, C, D, and E of fig. 4—all have a relatively consistent iron content that is a little lower than the value of 7.2 weight percent given for the northern highlands immediately west of the central far side. The far-side highlands are consistent with the southern highlands that are an extension of area E. Area A, coincident with the Mendeleev basin, has a lower iron content than the rest of the central far side, but the iron percent is comparable to, or higher than, that in the highlands extending from the Hertzsprung basin eastward across Orientale ejecta and Orientale's northern rim (Metzger and others, 1974). The Van de Graaff area has the highest iron content recorded on the far side. This is higher than the average terra value but lower than most maria and could be explained by its mare patches. Magnesium, unlike iron, does not seem to exhibit any pattern in the central far side, except that the values in the northern strip are a little lower than those in the southern strip; Van de Graaff falls in the middle. This contrasts with the general correlation of higher magnesium values over most maria relative to most terrae, but the correlation is not so marked or consistent as that of iron (Metzger and others, 1974, p. 1074, and table 3 and 4). As titanium values have been published for the southern ground tracks only, generalizations cannot be made. In the Van de Graaff area, however, the titanium values do seem to be too low for a typical mare. Finally, most values for potassium and thorium plus uranium, and the ratios between these elements, are consistent with the near-side terrae values. The values in the van de Graaff cell, however, appear similar to the near-side eastern maria, particularly Mare Serenitatis. The resolution cells for the eastern maria include areas of terra but not as much as in the Van de Graaff cell.

In summary, the gamma-ray data for the central far side show that all areas except Van de Graaff have chemical compositions comparable to other terrae areas. However, the resolution cells for most of the geochemical results are too large to pick up local variations in composition. The Van de Graaff cell is unique in its chemistry: iron, thorium plus uranium, and potassium contents are higher than typical terra and lower than most maria; magnesium and particularly titanium are too low for mare. Probably the chemical values reflect a mixture of materials that include terra, the grooved material (unit Ig), and some mare.

MAGNETIC DATA

Approximately 20 percent of the Moon's magnetic field has been mapped from orbital magnetometers by measuring the vector magnetic fields (Sharp and others, 1973; Russell and others, 1973, 1974, 1975). Most of the vector magnetic coverage is duplicated and also

extended by electron scattering measurements (Howe and others, 1974; McCoy and others, 1975, Lin and others, 1975; 1976; Anderson and others, 1976; R. P. Lin, unpub. data, 1976). Complementary work on a much coarser scale (10° x l0° resolution cells) has been compiled from measurements of solar wind compressions that are interpreted as being caused by the lunar magnetic field (Russell and Lichtenstein, 1975). A general conclusion based all these data sets is that the Moon is extensively magnetized in both the terrae and maria, but that magnetic anomalies are much more numerous in the terrae than in the maria. The strongest fields detected to this time occur on the far side (figs. 5 and 6). The main anomalies detected by the vector magnetic fields are also detected by the other two methods.

Four main magnetic anomalies are evident in figures 5 and 6 (centered at about 22° S. and 170° E., 20° S. and 170° W., 0° and 165° E., and 5° N. and 175° W.) and are apparent in Lin's electron scattering maps (Lin and others, 1975; R. P. Lin, unpub. data, 1976); Lin and others show a fifth anomaly (2° N. and 155° W.). The two southern anomalies are the strongest and could be considered as one large anomalous zone from the limb compression data and the electron scattering data. The western-most of these anomalies is near the crater Van de Graaff and is the largest anomaly so far detected on the Moon. The two anomalies appear distinct and separate on the vector field measurements (Sharp and others, 1973; Russell and others, 1974; figs. 5 and 6), and Russell and Lichtenstein (1975) also interpret their data as indicating two separate anomalies. The fine-scale plot of the Van de Graaff anomaly shows a highly structured field (Sharp and others, 1973, fig. 10) whose origin is still being debated (Sharp and others, 1973; Strangway and others, 1973; Stuart-Alexander, 1975).

Origin of all lunar magnetic anomalies is still in doubt. It is difficult to ascribe them to the surface geologic units because, at least in this map area, the units under each anomaly are diverse in origin and age: a pre-Nectarian crater, pre-Nectarian through Nectarian terra, a Nectarian basin, Imbrian grooved material, and ejecta blankets of early Imbrian craters. The only consistent relation discernible to me is that each anomaly is close to the major structural rim of an old basin. The southern anomalies are actually just within the proposed outermost rim of the South Pole–Aitken basin, although the western-most anomaly near Van de Graaff is also close to the outermost rim of the pre-Nectarian Keeler–Heaviside basin. The northern anomalies lie, from west to east, near the projection of the northern rim of Keeler-Heaviside basin, outside the southern rim of the pre-Nectarian Freundlich–Sharonov basin, and straddling the rim crest of the Nectarian Korolev basin. With the exception of Korolev, the youngest (Nectarian) basins in the mapped area—Mendeleev and Moscoviense—do not appear to have magnetic anomalies. Apollo, another of the old basins, was too far from the ground track to register, although Russell and Lichtenstein (1975) believe that the easternmost of their major anomalies is associated with that basin. Note that these anomalies, with the possible exception of South Pole–Aitken basin, occur along only small segments of the basin rims.

GRAVITY DATA

Computations of lunar gravity fields have been based on direct tracking from Earth of an orbiting spacecraft. Results for most of the near side were based on Lunar Orbiter data; computations for the far side were much more difficult. Two workers have recently made new attempts to combine the data from both Lunar Orbiter and Apollo spacecraft perturbations over the far side (Ferrari, 1975; Ananda, 1975; Ananda and Ferrari, 1975). There still appear to be problems in reducing the data. For instance, there is a periodicity in Ferrari's map that might be suspect; the positive anomalies appear in north-south bands, nicely balanced by parallel bands of negative anomalies. Ananda's data, on the other hand, show a more irregular distribution of positive and negative anomalies that is more comparable to the near-side reduction (see for example, Sjogren, 1974). The problem with the reduction is that the anomalies do not correlate directly with physical features on the ground but are commonly offset; the direction of offset may be consistent.

The map that combines the two reductions (Ananda and Ferrari, 1975, pl. 13) has made "Qualitative adjustments. . . to eliminate solution errors and to locate major anomalies over corresponding topographic features." Unfortunately, this map may have introduced other errors. It shows the Moscoviense and Mendeleev basins to be gravity lows of equal value, forcing some of Ananda's data to the west and some to the east, whereas Ananda's original map shows a positive anomaly centered slightly west of Moscoviense and a negative one equally offset to the west of Mendeleev. Because Moscoviense contains a significant quantity of mare rocks, the negative anomaly over it should be less than over Mendeleev in fact, the Moscoviense anomaly could well be positive. Additionally, the negative anomalies immediately east of Moscoviense and Mendeleev on Ananda's map coincide quite well with the Freundlich–Sharonov basin as mapped here. The revised Ananda-Ferrari map shows this area as strong gravity high, which is inconsistent with a "dry" basin, even a very old basin. Finally, the Ananda map generally shows the interbasin areas, particularly the old pre-Nectarian terra, as gravity highs. This consistent picture may be more nearly correct than the subsequent attempt to fit the data to certain basins, thereby missing others.

RADON-222 AND POLONIUM-210

Distribution of radon-222 and her delayed daughter polonium-210 was measured by Apollos 15 and 16 over approximately 15 percent of the Moon (Bjorkholm and others, 1973a, b). Because radon-222 is a decay product of uranium, the distribution of all three elements might be expected to be grossly parallel. Bjorkholm, Golub, and Gorenstein (1973a) maintain that this is so, but as they have published only one orbital path for radon-222 (1973a, fig. 1), their conclusion is not entirely supportable. They have published a map of the distribution of polonium-210 (1973b) on a 10° grid wherein the values vary from one place to another, but not in a consistent pattern. Apparently no particular signature differentiates mare from terra, whereas most of the other geophysical-geochemical measurements do. There is no readily discernible far-side/near-side distribution pattern and no apparent anomalies or the central far side.

INFRARED DATA

Apollo 17 flew an infrared scanning radiometer to measure thermal emission during lunar orbit. Preliminary analysis of the data (Low and Mendell, 1973) indicates that the Eratosthenian crater Birkland on the rim of Van de Graaff (lat 30° S., long 175° E.) has a slower cooling rate than the surrounding terrain. A second, smaller anomaly is adjacent to the Birkland ejecta blanket within Van de Graaff (Low and Mendell, 1973). Both of these anomalies are consistent with the findings on the near-side by Shorthill and Saari (1969) that show younger craters to have slower cooling rates than older craters.

A preliminary map of the infrared data that has been made of a 15° band for long 168° to 145° W. (Mendell, 1974) does not go far enough south to include Birkland crater. It does, however, include part of the double crater Van de Graaff where there are four bright, young, probably Copernican craters too small to be mapped here. These show up as anomalies on Mendell's map (1974). Four other small anomalies are apparent on his map (17° S. and 170° W., 19° S. and 163° W., 12° S. and 152° W., and 13° S. and 150° W.), and these too are over, or close to, bright sharp craters of Copernican age too small to be mapped here. From these results, it is clear that the infrared scanning technique and resultant maps are useful mapping tools for identifying young, fresh features and would be particularly helpful in areas where photography is poor.

CONCLUSIONS

For the central far side of the Moon, the pre-Nectarian and Nectarian were the most significant geologic periods, whereas on the near side, the Imbrian System dominates the geology. The decline in impact flux between the Nectarian and Imbrian Periods is clearly evident on the far side in the relative paucity of Imbrian and younger craters and by the

reduction in diameter of the largest craters in the three youngest systems. All of the central far-side basins are Nectarian or older, as are most of the other mapped materials. The basins are the structures that control the emplacement of most maria and apparently control the surface geochemical and geophysical properties of most areas. In particular, the giant depression of the southern hemisphere, here named the South Pole–Aitken basin, exerts a tremendous control over much of the geology of the central far side. It is the largest lunar basin whose structure is discernible by more than one parameter. It is one of the lowest areas on the Moon. Most of the far-side maria lie within its boundaries. Finally, the preponderance of all geologic, geochemical, and geophysical anomalies on the central far side lie within its boundaries; how much of this is coincidental (because of the huge size of the basin) is still uncertain.

Two extensive units may not be controlled by Nectarian or older basins. One is the light plains material (unit Ip), which is widespread over the area primarily as a filler in craters and other low areas. There is some indication of a concentration in the eastern half of the area, suggesting a possible relation to an Imbrian basin, possibly Orientale. The other is the enigmatic unit of grooves and mounds (Ig) that seems to be related to the formation of the Imbrium basin.

In general. the geochemical results are consistent with the typical near-side signatures that distinguish terrae from maria. Possible exceptions are the analyses over the part of the South Pole–Aitken basin that includes the crater Van de Graaff. There is a radioactive high in this region that could be related to maria under and adjacent to groundtracks of the orbiting spacecraft. Iron content is consistent with the percentage of maria present, whereas both magnesium and titanium seem low for maria. This supports the suggestion that part of the radioactive anomalies may be produced by some other material under the groundtrack, possibly the grooves and mounds (unit Ig).

The magnetic data appear very significant but are inconclusive. The highest anomaly so far detected on the Moon lies within the South Pole–Aitken basin, near the crater Van de Graaff, and another significant anomaly lies farther east in the basin. The geologic correlation with the three other significant magnetic anomalies on the far side may be their location near the outer ring of a major basin.

REFERENCES

Ananda, Mohan, 1975, Farside lunar gravity from a mass point model, Proc. 6th Lunar Sci. Conf.: Geochim. et Cosmochim. Acta, suppl. 6, v. 3, p. 2785–2796.

Ananda, M. P., and Ferrari, A. J., 1975, Lunar farside gravity, Proc 6th Lunar Sci Conf.: Geochim. et Cosmochim. Acta, suppl. 6, v. 3, Frontispiece, pl. 13.

Anderson, K. A., Lin, R. P., McCoy, J. E., McGuire, R. E., Russell, C. T., and Coleman, P. J., 1976, The large magnetized region associated with Rima Sirsalis, *in* Abstracts, 7th Lunar Sci. Conf.: Houston. Lunar Sci. Inst., p. 16–18.

Apollo 16 Preliminary Examination Team, 1973, The Apollo 16 Lunar Samples—petrographic and chemical description: Science, v. 179, p. 23–34.

Baldwin, R. B., 1969, Ancient giant craters and the age of the lunar surface: Astronom. Jour., v. 74, no. 4, p. 570–571.

Bills, B. G., and Ferrari, A. J., 1975, Lunar topography, Proc. 6th Lunar Sci. Conf.: Geochim. et Cosmochim. Acta, suppl. 6, v. 3, Frontispiece, pl. 2.

Bjorkholm, P. J., Golub, Leon, and Gorenstein, Paul, 1973a, Distribution of Rn-222 and Po-210 on the lunar surface as observed by the alpha particle spectrometer, Proc. 4th Lunar Sci. Conf.: Geochim. et Cosmochim. Acta, suppl. 4, v 3, p. 2793–2802.

_____1973b, Distributions of Polonium-2l0, Proc. 4th Lunar Sci. Conf.: Geochim. et Cosmochim. Acta, suppl 4, v. 1, Frontispiece, pl. 5.

Boyce, J. M., Dial, A. L., and Soderblom, L. A., 1974, Ages of the lunar nearside light plains and maria, Proc. 5th Lunar Sci Conf.: Geochim. et Cosmochim. Acta, Suppl. 5, v. 1, p. 11–23.

Campbell, M. J., O'Leary, B. T., and Sagan, Carl, 1969, Moon—Two new mascon basins: Science, v. 164, p. 1273–1275.

Carr, M. H., and El-Baz, Farouk, 1971, Geologic map of the Apennine-Hadley region of the Moon—Apollo 15 pre-mission map: U. S. Geol. Survey Misc. Inv. Map I-723 (sheet 1).

Chao, E. C. T., 1974, Impact cratering models and their application to lunar studies—a geologist's view, Proc. 5th Lunar Sci Conf: Geochim. et Cosmochim. Acta, suppl 5, v 1, p 35–52.

Eggleton, R. E., 1964, Preliminary geology of the Riphaeus quadrangle of the Moon and definition of the Fra Mauro Formation, *in* Astrogeologic Studies Ann. Prog. Rept., August 1962–July 1963, pt. A: U.S. Geol. Survey open-file report, p. 46–63.

_____1965, Geologic map of the Riphaeus Mountains region of the Moon: U.S. Geol. Survey Misc. Geol. Inv. Map I-458.

Eggleton, R. E., and Schaber, G. G., 1972, Cayley Formation interpreted as basin ejecta, *in* Apollo 16 preliminary science report: NASA SP-315, p. 29–7 to 29–16.

Eldridge, J. E., O'Kelley, G. D., and Northcutt, K. J., 1972, Abundances of primordial and cosmogenic radionuclides in Apollo 14 rocks and fines, Proc. 3rd Lunar Sci. Conf.: Geochim. et Cosmochim. Acta. suppl. 3, v. 2, p. 1651–1658.

Ferrari, A. J., 1975, Lunar gravity—the first farside map: Science, v. 188, p. 1297–1300.

Hartmann, W. K., and Kuiper, G. P., 1962, Concentric structures surrounding lunar basins: Arizona Univ. Lunar and Planetary Lab. Commun., v. 1, no. 12, p. 51–67.

Hartmann, W. K., and Wood, C. A., 1971, Moon—origin and evolution of multi-ring basins: The Moon, v. 3. p. 3–78.

Howard. K. A., Wilhelms, D. E., and Scott, D. H., 1974, Lunar basin formation and highlands stratigraphy: Reviews Geophys. and Space Physics, v. 12. no. 3, p. 309–327.

Howe, H. C., Lin, R. P., McGuire, R. E., and Anderson, K. A., 1974, Energetic electron scattering from the lunar remanent magnetic field: Geophys. Research Letters, v. 1, no. 3, p. 101–104.

Kaula, W. M., Schubert, G., Lingenfelter, R. E., Sjogren, W. L., and Wollenhaupt, W. R., 1973, Lunar, topography from Apollo 15 and 16 laser altimetry, Proc 4th Lunar Sci. Conf.: Geochim. et Cosmochim., Acta, suppl. 4, v. 3, p. 2811–2819.

Kinsler, D. C., Merrill, R. B., and Srnka, L. J., 1975, Apollo laser altimetry, Proc. 6th Lunar Sci. Conf.: Geochim. et Cosmochim. Acta, suppl. 6, v. 3, Frontispiece, pl. 1.

Lin R. P., Anderson, K. A., McGuire, R. E., and McCoy, J. E., 1976, Fine scale lunar surface magnetic fields detected by the electron reflection method, *in* Abstracts, 7th Lunar Sci. Conf.: Houston, Lunar Sci. Inst., p. 492–494.

Lin, R.P., McGuire, R.E., Howe, H.C., and Anderson, K.A., 1975, Mapping of lunar surface remanent magnetic fields by electron scattering, Proc. 6th Lunar Sci. Conf.: Geochim. et Cosmochim. Acta, suppl. 6. v. 3, p 2971–2973, and Frontispiece, pl. 3 and 4.

Low, F. J., and Mendell, W. W., 1973, Infrared scanning radiometer, *in* Apollo 17 preliminary science report: NASA SP-330, p. 24–1 to 24–6.

Markov, A. V., 1962, Description of the lunar surface, *in* A. V. Markov, ed., The Moon: Univ. Chicago Press, p. 75–99.

McCauley, J. F., 1967, The nature of the lunar surface as determined by systematic geologic mapping, *in* Runcorn, S. K., ed., Mantles of the Earth and terrestrial planets: New York and London, John Wiley & Sons, p. 431–460.

McCoy, J. E., Anderson, K. A., Lin, R. P., Howe, H. C., and McGuire, R. E., 1975, Lunar remanent magnetic field mapping from orbital observations of mirrored electrons: The Moon, v. 14, p. 35–47.

Mendell, W. W., 1974, Apollo 17 infrared scanning radiometer lunar farside radiance map, Proc. 5th Lunar Sci. Conf.: Geochim. et Cosmochim. Acta, suppl. 5, v. 1, Frontispiece, pl. l0.

Metzger, A. E., Trombka, J. I., Peterson, L. E., Reedy, R. C., and Arnold, J. R., 1973a, Lunar surface radioactivity—Preliminary results of the Apollo I5 and 16 gamma-ray spectrometer experiments: Science, v. 179, p. 800–803.

____1973b, Net lunar radioactivity, Proc. 4th Lunar Sci. Conf.: Geochim. et Cosmochim. Acta, suppl. 4, v. 1, Frontispiece, pl. 2.

Metzger, A. E., Trombka, J. I., Reedy, R. C., and Arnold, J. R., 1974, Element concentrations from lunar orbital gamma-ray measurements, Proc. 5th Lunar Sci. Conf.: Geochim. et Cosmochim. Acta, suppl. 5, v. 2, p. 1067–1078, and v. 1, Frontispiece, pl. 2.

Milton, D. J., and Hodges, C. A., 1972, Geologic maps of the Descartes region of the Moon—Apollo 16 pre-mission maps: U.S. Geol. Survey Misc. Inv. Map I-748.

Moore, H. J., Hodges, C. A., and Scott, D. H., 1974, Multiringed basins—illustrated by Orientale and associated features, Proc. 5th Lunar Sci. Conf.: Geochim. et Cosmochim. Acta, suppl. 5 v. l, p. 71–100.

Murray, B. C., Danielson, G. E., Davies, M. E., Gault, D. E., Hapke, Bruce, O'Leary, Brian, Strom R. G., Suomi, Verner, and Trask, Newell, 1974, Mercury's surface—preliminary description and interpretation from Mariner 10 pictures: Science, v. 185, p. 169–179.

Mutch, T. A., 1972, Geology of the Moon, a stratigraphic view: Princeton, N. J., Princeton Univ. Press, 2d ed., 391 p.

Oberbeck, V. R., Hörz, F., Morrison, R. H., Quaide, W. L., and Gault, D. E., 1975, On the origin of the lunar smooth-plains: The Moon, v. 12, p. 19–54.

Oberbeck, V. R., Morrison, R. H., Hörz, F., Quaide, W. L., and Gault, D. E., 1974, Smooth plains and continuous deposits of craters and basins, Proc. 5th Lunar Sci. Conf.: Geochim. et Cosmochim. Acta, suppl. 5, v. 1, p. 111–136.

Papanastassiou, D. A., and Wasserburg, G. J., 1973, Rb-Sr ages and initial strontium in basalts from Apollo 15: Earth and Planetary Sci. Letters, v. 17, p. 324–337.

Rodionov, B. N., Isavnina, I. V., Avdeev, Yu. F., Blagov, V. D., and others, 1971, New data on the Moon's figure and relief based on results from the reduction of Zond-6 photographs: Cosmic Research, v. 9, no. 3, p. 410–417.

Russell, C. T., Coleman, P. J., Jr., Lichenstein, B. R., Schubert, G., and Sharp, L. R., l973, subsatellite measurements of the lunar magnetic field, Proc. 4th Lunar Sci. Conf.: Geochim. et Cosmochim. Acta, suppl. 4, v. 3, p. 2833–2845.

Russell, C. T., Coleman, P. J., Jr., and Schubert, G. , 1974, Magnetic fields, Proc. 5th Lunar Sci. Conf.: Geochim. et Cosmochim. Acta, suppl. 5, v. 1, Frontispiece, pl. 3–8.

____1975, Magnetic fields, Proc. 6th Lunar Sci. Conf.: Geochim. et Cosmochim. Acta, suppl. 6, v. 3, Frontispiece, pl. 5–12.

Russell, C. T., and Lichenstein, B. R., 1975, on the source of lunar limb compressions: Jour. Geophys. Research, v. 80, p. 4700–4711.

Schultz, P. H., and Gault, D. E., 1975, Seismic effects from major basin formations on the Moon and Mercury: The Moon, v. 12, p. 159–177.

Scott, D. H., McCauley, J. F. and West, M. N., 1977, Geologic map of the west side of the Moon: U. S. Geol. Survey Misc. Geol. Inv. Map I-1034.

Sharp, L. R., Coleman, P. J., Jr., Lichenstein. B. R., Russell, C. T., and Schubert, G., 1973, Orbital mapping of the lunar magnetic field: The Moon, v. 7, no 3/4, p. 322–341.

Shoemaker, E. M., and Hackman, R. J., 1962, Stratigraphic basis for a lunar time scale, *in* Kopal, Zdenek, and Mikhailov, Z. K., eds., The Moon—Internat. Astron. Union Symposium 14, Leningrad 1960: London, Academic Press, p. 289–300.

Shorthill, R. W., and Saari, J. M., 1969, Infrared observations on the eclipsed Moon: Seattle, Wash., Boeing Sci. Research Labs. Doc. D1-82-0778, 73 p.

Sjogren, W. L., 1974, Lunar gravity at 100 km altitude, Proc. 5th Lunar Sci. Conf.: Geochim. et Cosmochim. Acta, suppl. 5, v. 1, Frontispiece, plate 1.

Soderblom, L. A., and Lebofsky, L. A., 1972, Technique for rapid determination of relative ages of lunar areas from orbital photography: Jour. Geophys. Research, v. 77, p. 279–296.

Strangway, D. W., Gose, W. A., Pearce, G. W., and McConnell, R. K., 1973, Lunar magnetic anomalies and the Cayley Formation: Nature, v. 246, p. 112–115.

Stuart-Alexander, D. E., 1975, Lunar magnetic anomalies and the Cayley Formation: Nature, v. 253, p. 658.

Stuart-Alexander, D. E., and Howard, K. A., 1970, Lunar maria and circular basins—a review: Icarus, v. 12, p. 440–456.

Stuart-Alexander, D. E., and Wilhelms, D. E., 1975, The Nectarian System, a new lunar time-stratigraphic unit: U.S. Geol. Survey Jour. Research, v. 3, no. 1, p. 53–58.

Tera, Fouad, Papanastassiou, D. A., and Wasserburg, G. J., 1974, Isototopic evidence for a terminal lunar cataclysm: Earth and Planetary Sci. Letters, v. 22, p. 121.

Trask, N. J., and McCauley, J. F., 1972, Differentiation and volcanism in the lunar highlands—photogeologic evidence and Apollo 16 implications: Earth and Planetary Sci. Letters, v. 14, p. 201–206.

Trombka, J. I., Arnold, J. R., Reedy, R. C., and Peterson, L. E., 1973, Some correlations between measurements by the Apollo gamma-ray spectrometer and other lunar observations, Proc. 4th Lunar Sci. Conf.: Geochim. et Cosmochim. Acta, suppl. 4, v. 3, p. 2847–2853.

Wilhelms, D. E., 1970, Summary of lunar stratigraphy—telescopic observations: U.S. Geol. Survey Prof. Paper 599-F, 47 p.

Wilhelms, D. E., and El-Baz, Farouk, 1977, Geologic map of the east side of the Moon: U.S. Geol. Survey Misc. Geol. Inv. Map I-948.

Wilhelms, D. E., and McCauley, J. F., 1971, Geologic map of the near side of the Moon: U.S. Geol. Survey Misc. Geol. Inv. Map I-703.

Wilhelms, D. E., Stuart-Alexander, D. E., and Howard, K. A., 1969, Preliminary interpretations of lunar geology, *in* Analysis of Apollo 8 photography and visual observations: NASA SP-201, p. 16–21.

Wollenhaupt, W. R., and Sjogren, W. L., 1972a, Comments on the figure of the Moon based on preliminary results from laser altimetry: The Moon, v. 4. no. 3/4. p. 337–347.

_____1972b, Apollo 16 laser altimeter, *in* Apollo 16 preliminary science report, NASA SP-315, p. 30–1 to 30–5.

Wollenhaupt, W. R., Sjogren, W. L., Lingrenfelter, R. E., Schubert, G, and Kaula, W. M., 1973, Apollo 17 laser altimeter, *in* Apollo 17 preliminary science report: NASA SP-330, p. 33–41 to 33–44.

Primary data source, NASA Lunar Orbiter moderate-resolution photographs (shown on index map). High resolution frames lie within moderate-resolution frames and were supplementary data source; they were main data for frame 30. Zond 8 (USSR) and Apollo 15, 16, and 17 photographs supplementary.

Work performed on behalf of the National Aeronautics and Space Administration under Contract No. W-13,130.

Part of shaded-relief base chart Lunar Farside Chart (LMP-2), 2d ed., October 1970, prepared by Defense Mapping Agency, Aerospace Center (formerly Aeronautical Chart and Information Center, U.S. Air Force), St. Louis, MO, 60318. The lunar surface features shown on this chart were interpreted from the photographic records of Lunar Orbiter Missions, I, II, III, IV, and V. Ray patterns and albedo differences are incomplete, owing to limitations of the source photographs. Horizontal positions of the features based on ACIC Positional Reference System, 1969. Feature names were taken from the International Astronomical Union list of 1970.

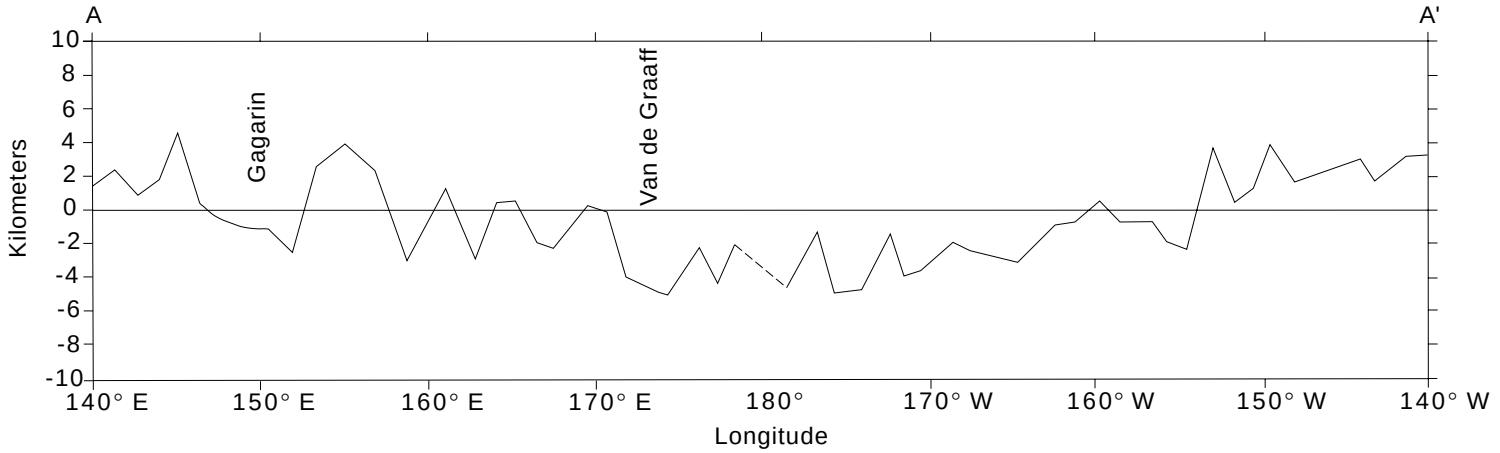

FIGURE 1.—Altitude profile across southern section of map (line A-A'). The major depressed area is the South Pole-Aitken basin. (Apollo 15 lunar altimetry, adapted from Wollenhaupt and Sjogren, 1972a, fig. 2a. Vertical exaggeration 30X.)

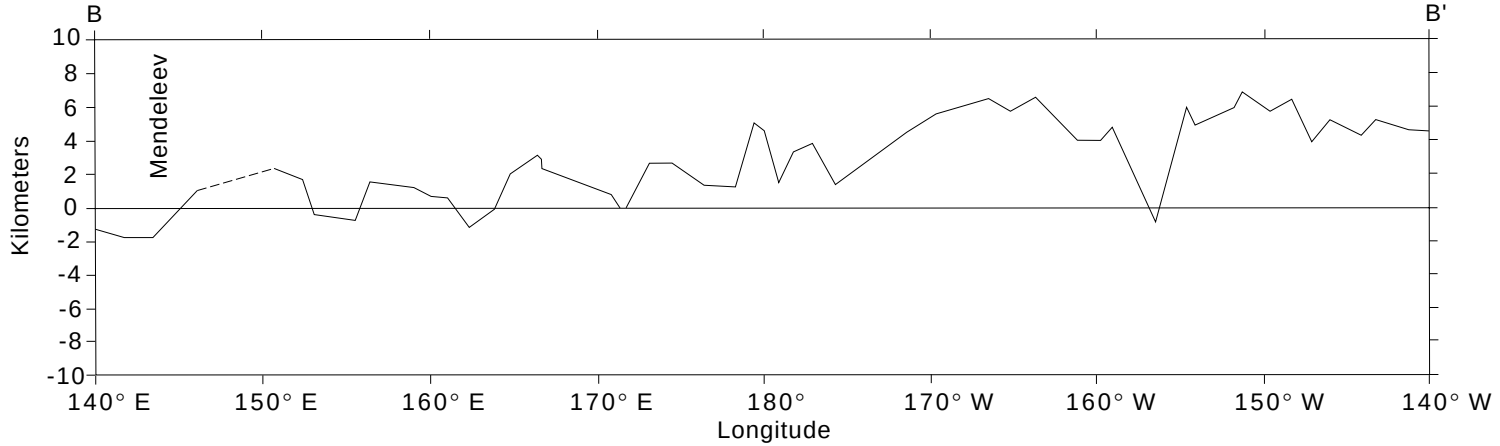

FIGURE 2.—Altitude profile across northern part of map (line B-B'). The sharp dip at 157° W. seems anomalously low for any crater in that area and so may be an error. (Apollo 16 laser altimetry, adapted from Wollenhaupt and Sjogren, 1972b, fig. 30-2a. Vertical exaggeration 30X.)

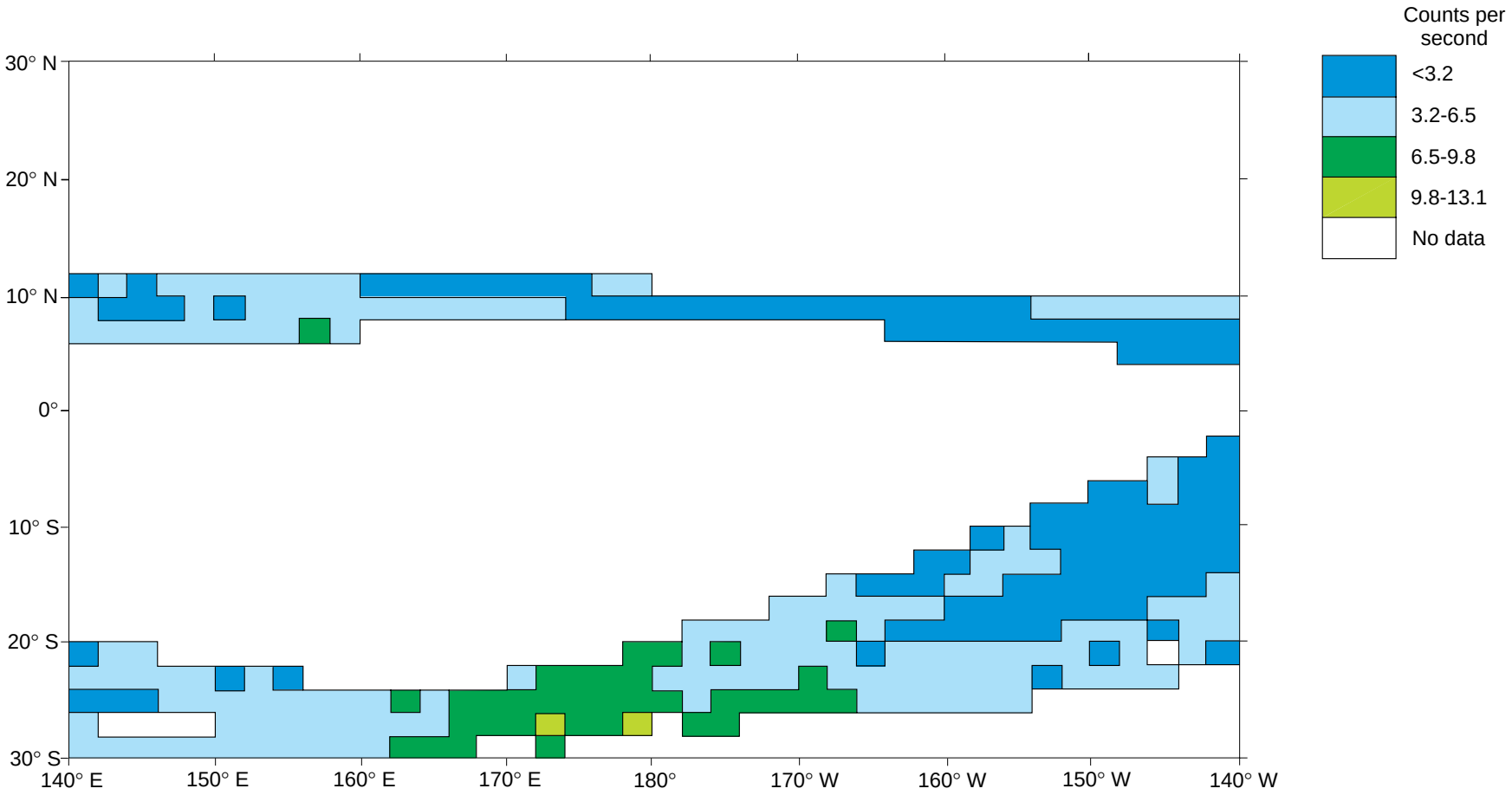

FIGURE 3.—Net lunar radioactivity of the areas flown over by Apollo 15 and 16 (Metzger and others, 1973b, pl. 2).

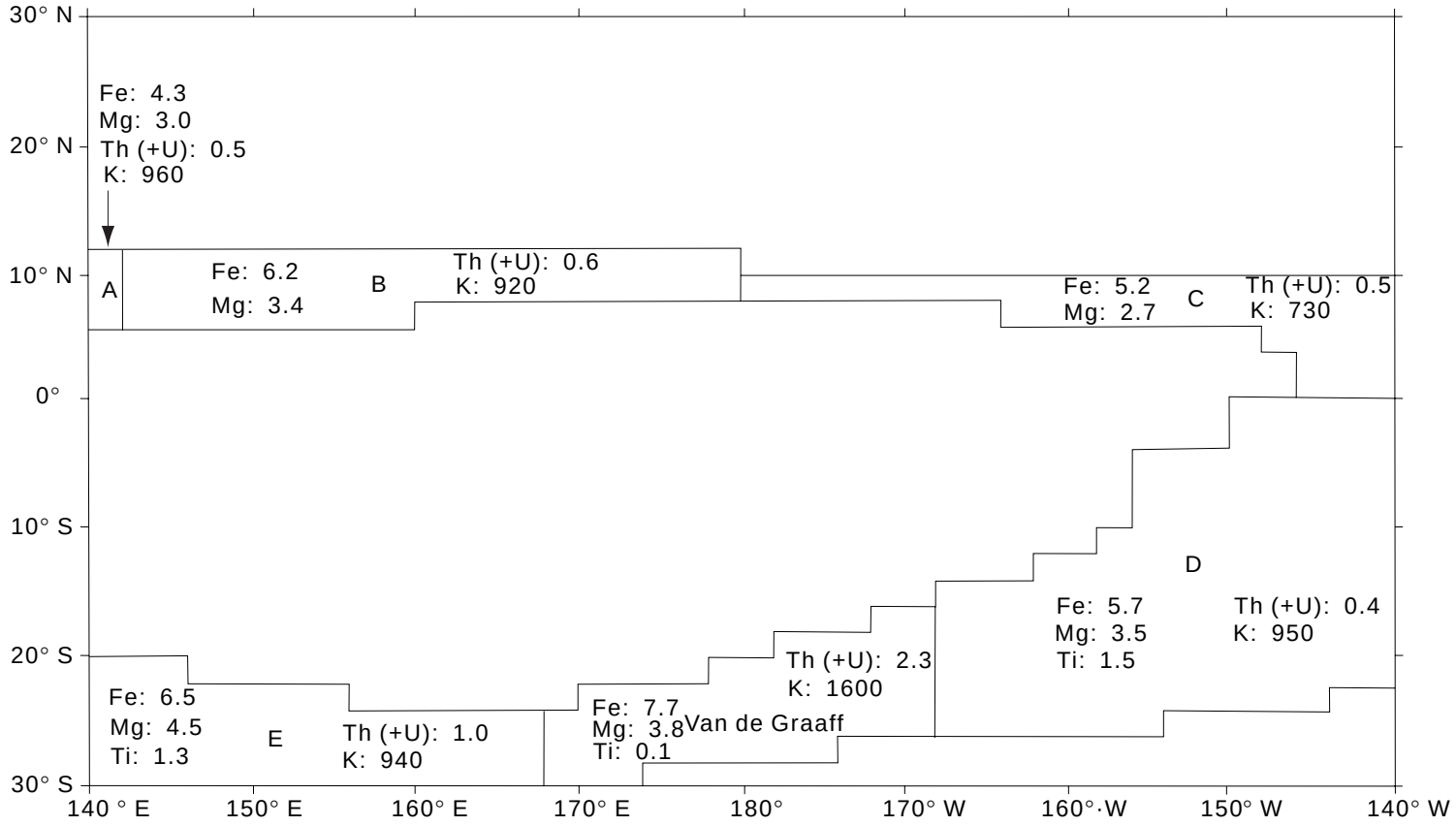

FIGURE 4. — Resolution cells for concentrations of chemical elements determined from the gamma-ray experiments of Apollo spacecraft (Metzger and others, 1974, from fig. 2., p. 1072). Iron, magnesium, and titanium given in weight percent; thorium plus uranium and potassium in parts per million.

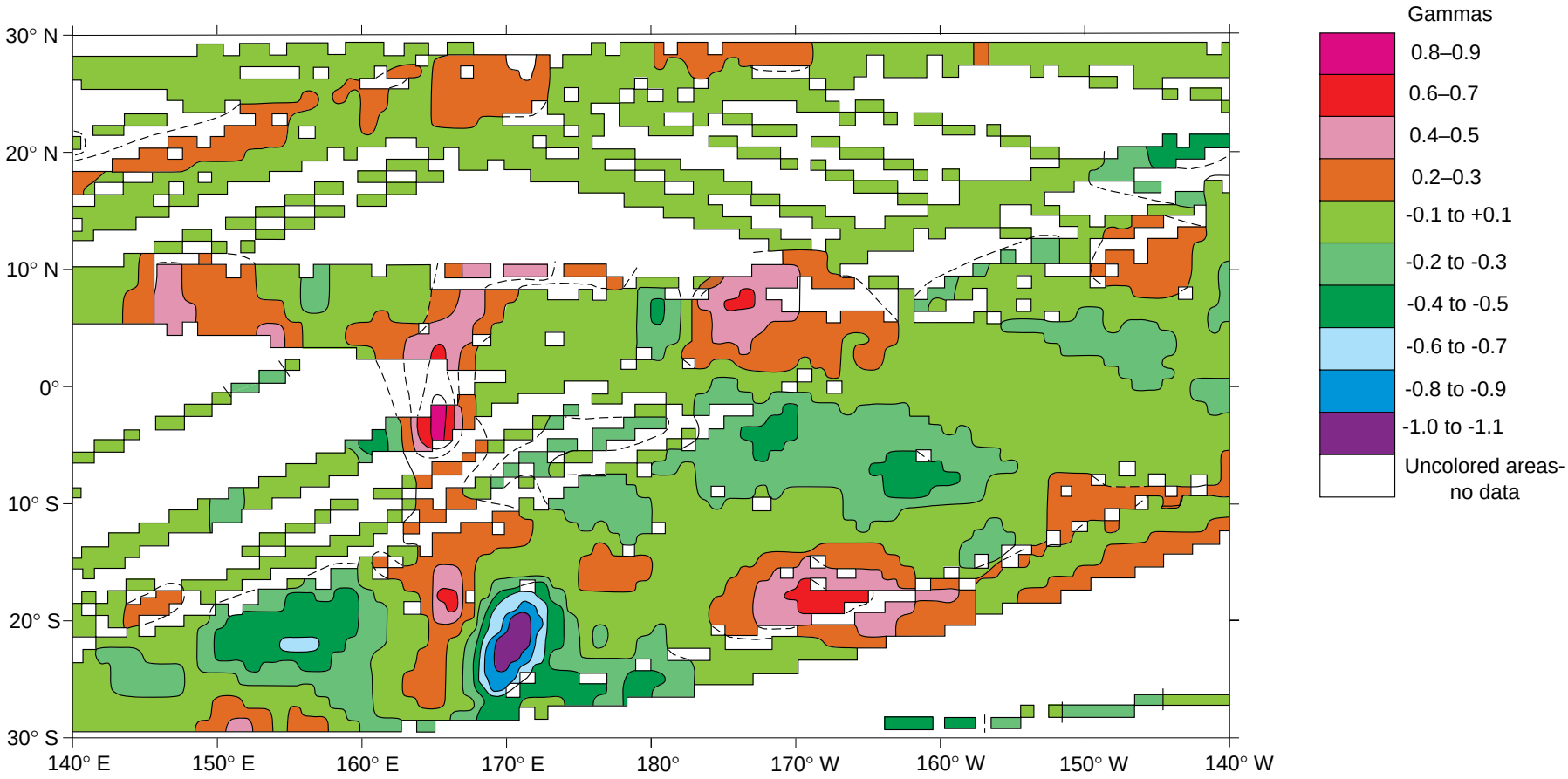

Figure 5.—Radial component of the magnetic field using all the data obtained from the subsatellite magnetometers of Apollos 15 and 16. Plus values are directed radially into the Moon. (Contoured by the author from data supplied by R.L. Sharp, Univ. California, Los Angeles, 1973. Sharp had normalized the data to an altitude of 100 km and derived values by averaging the field vector for each orbit in solar ecliptic coordinates and subtracting the average field from the individual vector measurements.)

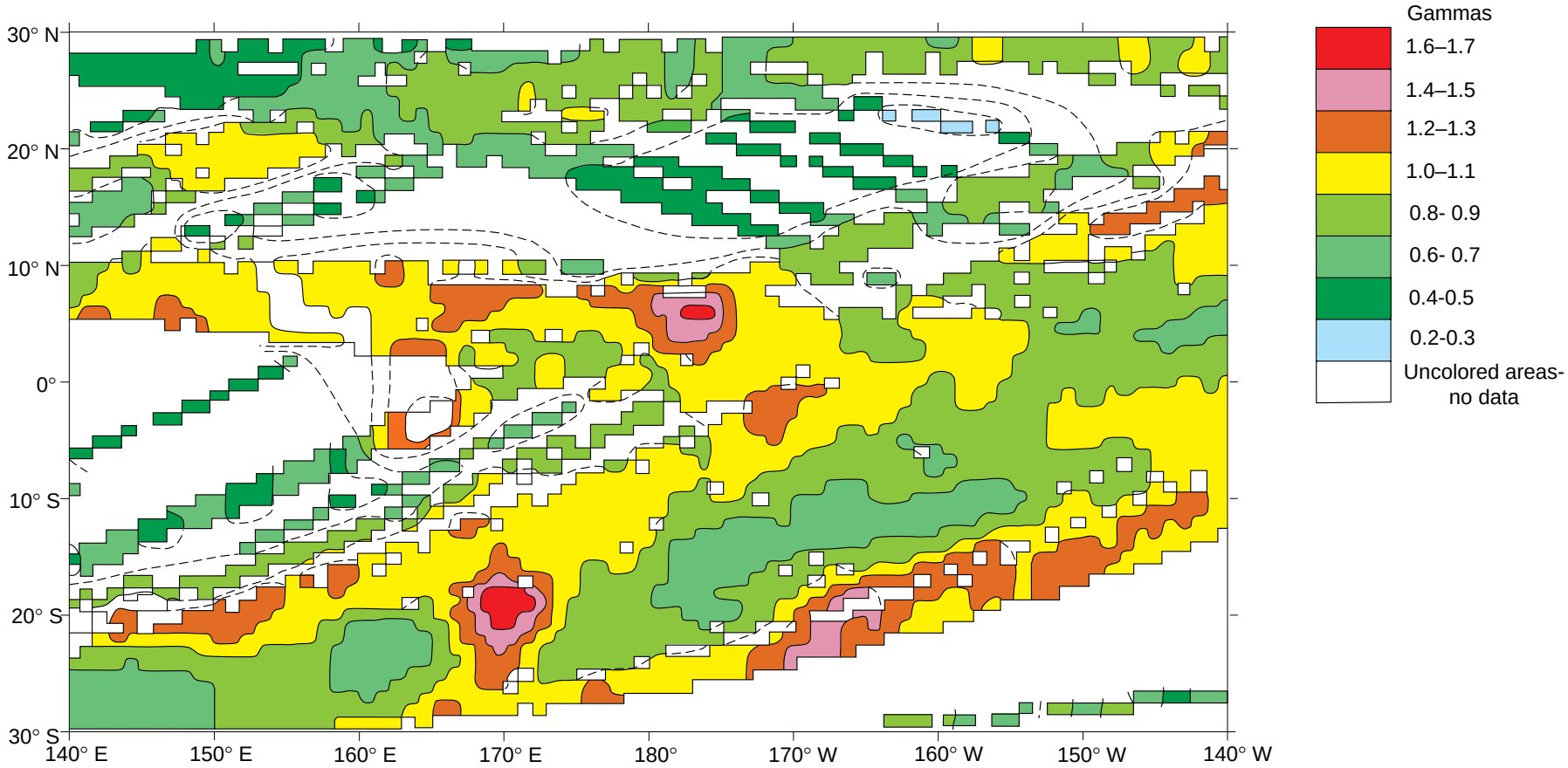

Figure 6.—Total magnetic field. Source and treatment of the data as in fig. 5.

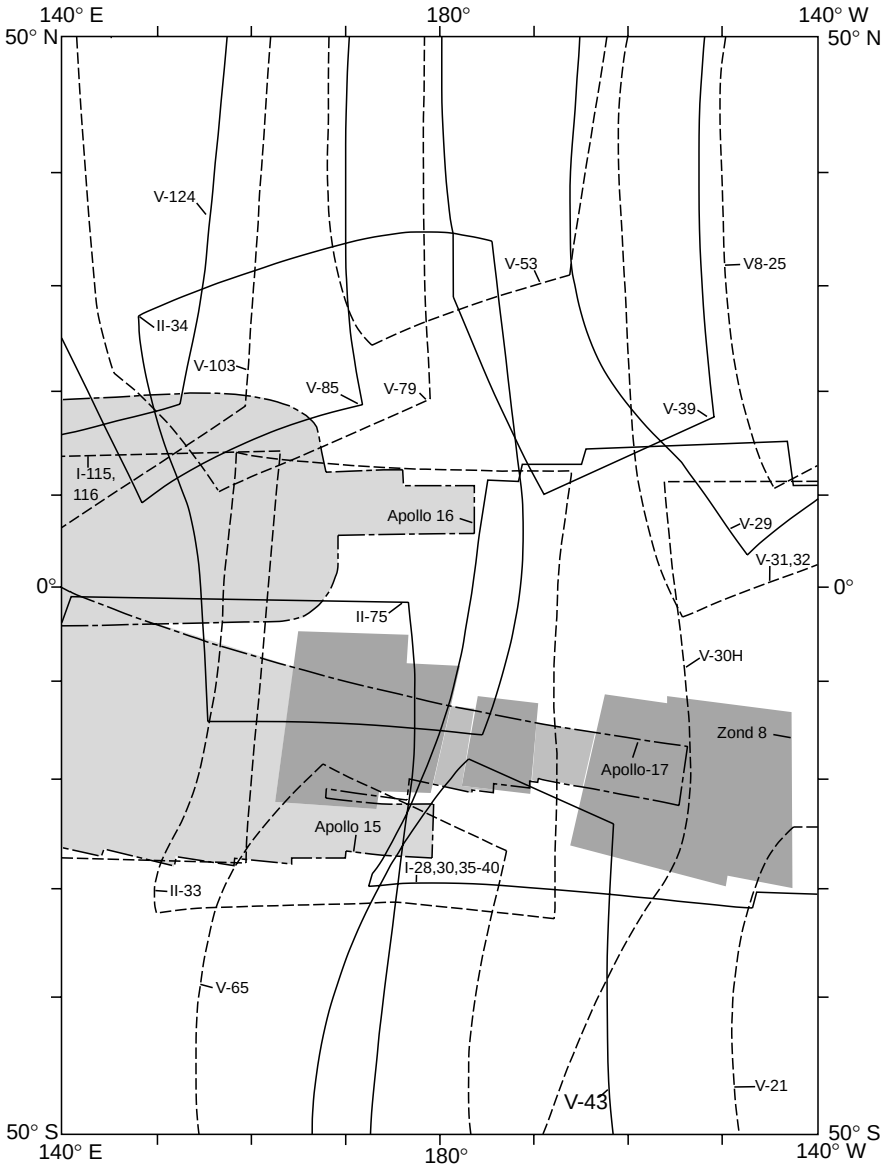

INDEX TO PHOTOGRAPHIC COVERAGE

Line-style alternated for clarity. Roman numerals are Lunar Orbiter mission numbers; Arabic numerals, frame numbers; H, high-resolution photograph. Zond 8, heavy shading; Apollo 15, 16, and 17, light shading. Outlines represent limits of useful coverage.

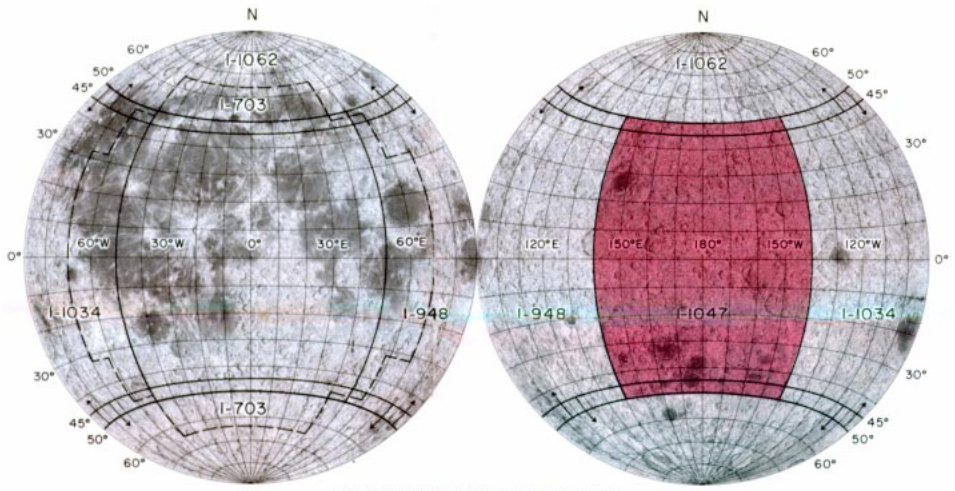

INDEX MAP OF THE MOON

The number preceded by I refers to published 1:5,000,000 geologic map

I-703	Geologic map of the Near Side of the Moon (dashed line)
I-948	Geologic map of the East Side of the Moon
I-1034	Geologic map of the West Side of the Moon
I-1047	Geologic map of the Central Far Side of the Moon
I-1062	Geologic map of the North Side of the Moon

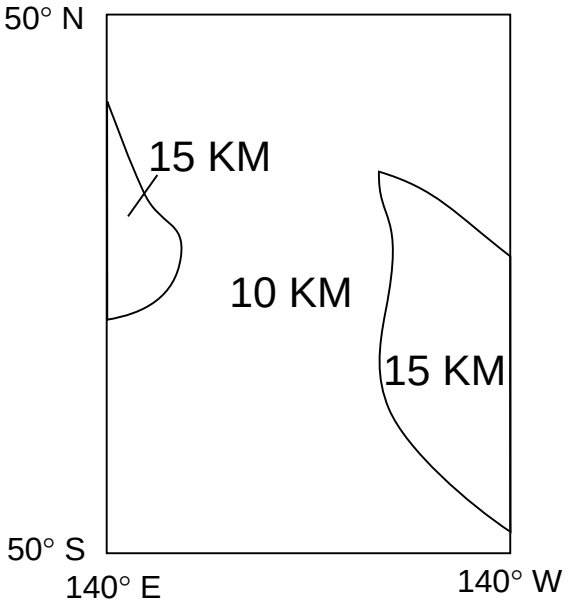

HORIZONTAL RELIABILITY
OF BASE MAP